BOAR: Biprism based Optical Autocorrelation with Retrieval

F. Billard, A. Dubrouil, E. Hertz, S Lecorné, E Szmygel, O. Faucher, P. Béjot

BOAR: Biprism based Optical Autocorrelation with Retrieval

F. Billard,[1] A. Dubrouil,[2] E. Hertz,[1] S. Lecorné,[2] E. Szmygel,[2] O. Faucher,[1] and P. Béjot[1, a)]
[1)] *Laboratoire Interdisciplinaire CARNOT de Bourgogne, UMR 6303 CNRS-Université Bourgogne Franche-Comté, 9 Av. A. Savary, BP 47870, F-21078 DIJON Cedex, France*
[2)] *FemtoEasy, Batiment Sonora, Parc scientifique et technologique Laseris 1, Avenue du Medoc 33114 Le Barp, France*

A simple and compact single-shot autocorrelator is presented and analyzed in details. The autocorrelator is composed of two elements only: a Fresnel biprism used to create two temporally-delayed replicas of the pulse to characterize and a camera in which two-photon absorption takes place. The two-photon absorption signal obtained in the camera can be used to retrieve the pulse duration, the frequency chirp, and the pulse spectrum provided that a gaussian temporal shape is assumed. Thanks to its extreme simplicity, the autocorrelator is robust and easy to align. As it does not use any nonlinear crystal, its spectral working range is very broad (1200-2400 nm). The presented design can characterize pulse duration from 25 fs to 1.5 ps. Nevertheless, it is shown that using a NaCl biprism instead should allow to measure pulse duration down to 12 fs. Finally, a proof-of-principle demonstration is also performed in a wavelength range located further in the infrared (1800-3400 nm) by using a InGaAs camera.

I. INTRODUCTION

The apparition of mode-locked lasers in the mid-60s raised the problem of ultrashort laser pulse characterization. Since the characteristic time scale of electronic was overwhelmed, optical techniques had to be developed. Ultrafast lasers kept evolving and the need for characterization increased with the performances of the lasers. A breakthrough was made when the Chirp Pulse Amplification lasers appeared and over the past three decades, ultrashort laser pulse characterization has been a major concern for laser physicists. Substantial effort are still made to develop and improve multitudinous techniques of characterization[1–3]. Indeed, the optical pulses characterization is a rather complex problem that is highly dependent on the lasers characteristics. There are many different approaches and each of them having advantages and drawbacks. The choice of a techniques has to be made in consideration of the laser experimental conditions. As the research in the field has been very active, there is numerous different techniques of characterization and some of them are very atypical[4–21]. We present here, a new technique for ultrashort pulses characterization based on single shot interferometric autocorrelation and two photon absorption. The devices and technique are so called, Biprism based Optical Autocorrelation with Retrieval (BOAR). It is a simple and compact single shot autocorrelator composed by only two elements: a Fresnel biprism and a camera. The latter is used to detect incident photon with energy lower than its absorption band gap, the only way to produce a signal is therefore to absorb two photons. This two-photon signal is a spatial interferogram that can be used to retrieve the pulse duration, the frequency chirp and the pulse spectrum. There is no non-linear crystal and no phase matching issues, the spectral working range is therefore very broad (1200-2400 nm with a silicon based camera and 1800-3400 nm with an InGaAs camera). For the sake of brevity, we compare here our technique with the most common ones (Autocorrelation[13,22–24], FROGs[12,25–34] and Spectral Interferometry[35–44]), and more atypical ones that are related to our technique[18,21,31,45–52]. Although autocorrelation needs an assumption on the temporal profile and it does not provide the exact pulse duration, it is the most simple and most robust technique, and therefore it is still widely used. Our technique is even more simple and more robust than an usual autocorrelator, although it allows to estimate the spectral phase and amplitude just like a FROG or a SPIDER. Spectrographic techniques like FROGs have a large working range and are suitable for complex and very chirped pulses[2,29,30]. They also have the advantage to be intuitive since an experienced user is able to estimate the chirp and its order just by looking at the frog trace. The disadvantage of FROGs is the heavy iterative algorithm that is needed to retrieve the phase. However it is still possible to retrieve the phase in real time[53] and some more powerful retrieval methods have recently appeared[2,54,55]. Spectral phase interferometry based technique like SPIDER[35] or SRSI[56] have the advantage to retrieve the phase by direct Fourier Transform calculation. However, the working range is very narrow and measurements are possible only when the pulse duration are not too far from the Fourier limit. The BOAR is actually combining all advantages: as an autocorrelator, it is therefore extremely robust, it is suitable for rather chirped pulses and the retrieval is done directly by Fourier transformation of the interferogram in the time domain (*i.e.*, an interferogram with encoded time). However the retrieval is direct and rapid if a Gaussian spectral profile is assumed, otherwise the calculations becomes heavier. Also BOAR relies on a single shot device and therefore it makes an important difference on the accessible information compared to multishot devices. The latter gives only an average measurement in time (on all the pulses required to obtain a measurement) and an average measurement in space[57] (the

[a)] Electronic mail: pierre.bejot@u-bourgogne.fr

beam is focused in multishot devices). On the contrary, single shot devices allow to access to pulse to pulse fluctuations and in this case the measurement is also spatially resolved[58–60]. It is therefore a pertinent information to evaluate the quality and stability of a laser system. Furthermore, it is known that the proper way to characterize stability performances is on a single shot basis[61–64]. In the following, we present the conception of the BOAR and the associated theory, experimental measurements, and numerical simulations. The latter are compared with the experimental data and then are used to determine the working range of the BOAR, the validity and accuracy of the results according to the experimental conditions.

II. BASIC PRINCIPLES OF THE BOAR

The Biprism based Optical Autocorrelator with Retrieval (BOAR) relies on two basic principles: the creation of two identical temporally delayed sub-pulses from the pulse to be measured and a nonlinear optical effect. These two steps are respectively performed with a Fresnel biprism and a camera in which two-photon absorption occurs. The combination of these two elements makes the BOAR extremely compact, calibration-free and robust in alignment.

A. Geometrical considerations

Figure 1(a) illustrates the basic principle of the autocorrelator. The creation of the two replica is performed by means of a Fresnel biprism having an Apex angle A, a refractive index n, a thickness e_0, and a height H (it will be supposed hereafter that the laser beam is larger than the biprism, i.e., that the biprism is the pupil of the optical system). The propagation of the laser pulse in the biprism leads to the creation of two identical beams crossing with an angle 2α in a plane parallel to the biprism input face, where $\alpha = \mathrm{asin}\left[n\mathrm{sin}\beta\right] - \beta$ and $\beta = \pi/2 - A/2$. The optical path difference of the two beams imposes a temporal delay given in first approximation by $\Delta\tau = \frac{2x\mathrm{sin}\alpha}{c}$, where x is the distance relative to the propagation axis z. The temporal information is then directly transposed in the spatial domain, then allowing single-shot pulse duration measurements, provided that the integration times of the camera is shorter than the repetition period of the laser to be measured. The optimal distance d_{opt} at which the two beams perfectly spatially overlap is given by: $d_{\mathrm{opt}} = \frac{H}{4}\left(\frac{1}{\mathrm{tan}\alpha} - \mathrm{tan}\beta\right)$. At this optimal distance, the temporal window $\Delta\tau_{\mathrm{max}}$ is given by: $\Delta\tau_{\mathrm{max}} = \frac{H}{c}\mathrm{sin}\alpha\left(1 - \mathrm{tan}\alpha\,\mathrm{tan}\beta\right)$. Note that these formula are obtained assuming that the laser pulse propagates at phase velocity in both the biprism and air, which leads to slightly underestimate the pulse duration. This can be corrected by applying a proportionality factor $\kappa = 1 + \frac{\omega_0 \mathrm{cos}\alpha}{n\mathrm{cos}\alpha - 1}\frac{\partial n}{\partial \omega}$ to the retrieved pulse duration

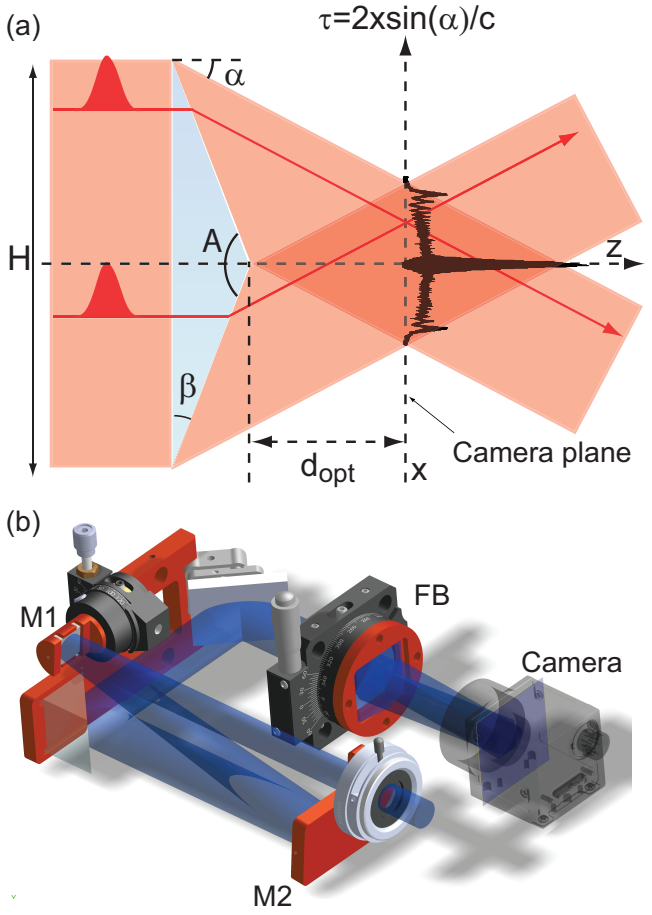

Figure 1. (a) Principle of the autocorrelator BOAR device. The black line is a typical experimental two-photon absorption signal recorded by the camera. (b) Experimental setup. The two cylindrical mirrors M_1 and M_2 ($f = -25\,\mathrm{mm}$ and $f = 125\,\mathrm{mm}$, respectively) are used for increasing the beam size in the horizontal direction by a factor of 5 and FB is the Fresnel biprism.

that takes into account the fact that the pulse envelope propagates at the group velocity.

B. Two-photon absorption

1. General formulas

The optical autocorrelation is performed by two-photon absorption in a camera having a pixel size dx and a number of pixels N along x placed at the distance d from the biprism output. The bandgap U_{g} of the semiconductor material composing the camera pixels is chosen in the interval $\frac{hc}{\lambda} < U_{\mathrm{g}} < 2\frac{hc}{\lambda}$, where h is the Planck constant, c is the light celerity, and λ is the central wavelength to be measured. For instance, a silicon (resp. InGaAs) camera ($U_{\mathrm{g}} = 1.11\,\mathrm{eV}$) can be used for measuring pulse duration in the [1200-2400 nm] (resp. [1800-3400 nm]) spectral range.

Considering the total complex electric field $\varepsilon(t,\tau) = \varepsilon_1(t) + \varepsilon_2(t-\tau)$ hitting a pixel of the camera, where $\varepsilon_1(t) = A_1(t)\mathrm{e}^{i\omega_0 t}$ (resp. $\varepsilon_2(t) = A_2(t)\mathrm{e}^{i\omega_0 t}$) is the field at frequency $\omega_0 = 2\pi c/\lambda$ coming from the upward (resp. downward) face of the biprism, the photocurrent I_{phot} induced by two-photon absorption in one pixel of the camera will is:

$$I_{\mathrm{phot}}(\tau) \propto \int |\varepsilon^2(t,\tau)|^2 dt. \quad (1)$$

Assuming a perfect balance between the two replicas amplitudes ($A_1 = A_2 = A$), the photocurrent is given by:

$$I_{\mathrm{phot}}(\tau) \propto G_2(\tau) + F_1(\tau)\cos(\omega_0\tau) + F_2(\tau)\cos(2\omega_0\tau), \quad (2)$$

where

$$\begin{aligned} G_2 &= 2\int I^2(t)dt + 4\int I(t)I(t-\tau)dt, \\ F_1 &= 4\int \left[I(t) + I(t-\tau)\right] \mathcal{R}e\left[A(t)A^*(t-\tau)\right] dt, \\ F_2 &= 2\int \mathcal{R}e\left(A^2(t)A^{*2}(t-\tau)\right) dt, \end{aligned} \quad (3)$$

and where $I = |A|^2$ is the field intensity. The contributions G_2, F_1, and F_2 oscillate at very different frequencies (ω=0, ω_0, and $2\,\omega_0$, respectively). Therefore, their relative contributions to the two-photon signal I_{phot} can be easily distinguished by an appropriate frequency filtering. One has to emphasize that the two-photon absorption signal then can be used to determine the central frequency of the laser to be measured provided that the optical characteristics of the biprism (Apex angle and refractive index) are well determined. Note that, since a part of the autocorrelation evolves with a frequency around $2\omega_0$, this imposes an upper limit on the spatial resolution of the optical system. Indeed, for resolving F_2, the camera pixel size has, at least, to be smaller than four times the interference period, i.e.,

$$dx \leq \lambda_0/(8\mathrm{sin}\alpha). \quad (4)$$

2. Autocorrelation measurement assuming chirped gaussian pulses

As every autocorrelator, an assumption about the temporal shape of the pulse has to be done so as to retrieve the pulse duration from the measurement. One of the widely used assumption is to consider a gaussian profile, possibly with a quadratic spectral phase. More particularly, if one imposes a quadratic spectral phase $\Phi(\omega) = K\omega^2$ on a Gaussian electric field with an envelope $A(t) = \mathrm{e}^{\frac{-t^2}{\sigma_t^2}}$ (and its associated spectral amplitude $\widetilde{A}(\omega) \propto \mathrm{e}^{\frac{-\sigma_t^2 w^2}{4}}$), the electric field complex envelope becomes:

$$A(t) = \mathrm{e}^{\frac{-t^2}{\sigma_{t_c}^2}}\mathrm{e}^{-iat^2}, \quad (5)$$

with $\sigma_{t_c} = \frac{\sqrt{\sigma_t^4+16K^2}}{\sigma_t}$ and $a = -4\frac{K}{\sigma_t^4+16K^2}$. According to these definitions, σ_t (resp. σ_{t_c} corresponds to the Fourier-Transformed limited (resp. effective) pulse duration, and a is the temporal phase. In this case, G_2, F_1, and F_2 reads respectively:

$$\begin{aligned} G_2(\tau) &= 1 + 2\mathrm{e}^{-\frac{\tau^2}{\sigma_{t_c}^2}}, \\ F_1(\tau) &= 4\cos\frac{a\tau^2}{2}\mathrm{e}^{-\frac{\tau^2}{2}\left(\frac{1}{\sigma_{t_c}^2}+\frac{1}{2\sigma_t^2}\right)}, \\ F_2(\tau) &= \mathrm{e}^{-\frac{\tau^2}{\sigma_t^2}}. \end{aligned} \quad (6)$$

A few remarks can then be done regarding the above expressions. First, the low-frequency part of the autocorrelation (G_2) gives access to the chirped pulse duration. However, a chirped pulse and a Fourier-Transform limited pulse with same duration produce the same signal for G_2. Note that G_2 embeds an offset induced by the two-photon absorption signal produced by the two replicas taken individually. As discussed below, the presence of this offset can be detrimental for an accurate fit of the pulse duration. Secondly, the contribution oscillating around $2\,\omega_0$ (F_2) is insensitive to the chirp and gives access to the unchirped pulse duration. More particularly, the amplitude of the Fourier Transform of F_2 corresponds to the field spectrum amplitude. Finally, the contribution F_1 oscillating around ω_0 is sensitive to both the pulse duration and the chirp. This function, however, is ill-suited in the case of highly chirped pulses. Indeed, this function tends to a distribution that is independent on the chirp applied to the field:

$$F_1(\tau) \underset{K\to\infty}{\sim} \mathrm{e}^{-\frac{\tau^2}{4\sigma_t^2}}. \quad (7)$$

As a consequence, particular care must be taken if one uses this function for retrieving the effective pulse duration, in particular if the spatial profile of the beam is noisy.

To conclude, the pulse duration can be retrieved in two different ways. The first method consists to fit G_2. The drawback of this measurement lies in the fact that this contribution is very sensitive to the quality of the beam profile. Indeed, since this contribution is a low-frequency oscillating function, almost all the noise coming from the beam shape imperfections is transferred on it. Moreover, the knowledge of G_2 does not provide any information on the frequency chirp. The second method is to use the combination of F_1 and F_2. First, the Fourier-Transform limited pulse duration is retrieved by fitting F_2, which also gives the pulse spectrum as described above. Then, the absolute value of the chirp parameter K, and consequently, the chirped pulse duration, can be determined by fitting F_1. As mentioned above, the determination of K is limited to moderate chirps most currently encountered in real experiments. Note that the two methods can be performed simultaneously and independently, improving then the accuracy of the measurement.

III. EXPERIMENTAL SETUP AND RESULTS

The optical design of the autocorrelator is depicted in Fig. 1(b). Before the Fresnel biprism, a cylindrical reflective telescope, composed by two cylindrical mirrors ($f = -25$ mm and $f = 125$ mm, respectively) increases the beam size by a factor of 5 in the horizontal direction, direction on which the pulse duration measurement is performed. The telescope ensures that the beam size does not limit the range of pulse durations that can be measured by the autocorrelator. Then, a A=160° 1.7 mm thick fused silica biprism (Newlight Photonics) is mounted in a manual rotation stage. Using this biprism and after correction coming from the difference between phase and group velocities, the total delay range $\Delta\tau_{\max}$ is then $\Delta\tau_{\max} \simeq 5.5$ ps and the optimal distance is $d_{\text{opt}} = 6.3$ cm. The camera used in the autocorrelator is a 12 bits silicon CMOS camera (Basler acA3800-14um). The minimal integration time is 35 μs, which makes the autocorrelator single-shot for lasers with a repetition rate lower than 28 kHz. The camera can be externally triggered with a 14 Hz maximal frame rate. The pixel size of the camera is dx=1.67 μm, which fulfills the condition given in Eq. 4 in the whole spectral range of interest. In the horizontal direction, the camera has 3840 pixels, which gives a 6.4 mm sensor size. Accordingly, the total delay range accessible with the present camera is only 3.5 ps, while the upper limit imposed by the biprism is 5.5 ps. As a consequence, since the camera field of view actually limits the delay range, the biprism was placed at a distance $d = 4.7$ cm, i.e. before d_{opt}. The rotation of the biprism is adjusted by aligning the interference fringes along the vertical dimension of the camera. The signal is transferred by USB 3.0 to a computer for further processing. While the refractive index of the material composing the biprism (in the present case, fused silica) is well known, the calibration of the Apex angle has been accurately performed prior to any autocorrelation measurements by illuminating the optical system with a HeNe laser and by measuring the interferences fringes spacing on the camera. The calibration procedure finally led to $A = 160.220° \pm 0.005°$. The laser characterized during the experiment is a commercial non-collinear optical parametric amplifier pumped by a 100 fs 800 nm chirped pulse amplified laser and delivers femtosecond laser pulses in the [1200-2400 nm] wavelength region. Figure 2(a) shows a typical signal recorded with the autocorrelator for a laser wavelength set at λ_0=2020 nm. A fast Fourier transform along the horizontal dimension allows to easily separate the three oscillating functions G_2, F_1 and F_2 that are shown in Figs. 2 (b-d). At the same time, knowing that F_1 and F_2 oscillates around ω_0 and $2\,\omega_0$ respectively, the central wavelength of the laser is estimated to be $\lambda_e = 2022$ nm, in very good agreement with the expectations. The retrieval procedure applied to G_2 gives a pulse duration (FWHM) $\Delta t \simeq 76$ fs. Using F_1 and F_2, one obtains $\Delta t \simeq 77$ fs (in very good agreement with the result obtained with G_2), a Fourier-Transform limited pulse duration $\Delta t_{\text{FTL}} \simeq 57$ fs and a group delay dispersion (GDD) of ± 1050 fs^2. Then, the same procedure has been performed after having inserted a 1.4 cm thick BK7 plate in the laser path [Figs. 2(b-d)]. As expected, the contribution oscillating around $2\omega_0$ remains unchanged while both G_2 and F_1 gets broader than in the case without the plate. The fit of G_2 leads to $\Delta t \simeq 137$ fs while those of F_1 and F_2 leads to $\Delta t \simeq 145$ fs, a Fourier-Transform limited pulse duration $\Delta t_{\text{FTL}} \simeq 56.7$ fs and a group delay dispersion (GDD) of ± 2720 fs^2. Accordingly, one can estimate that the GDD introduced by the BK7 plate is about 1670 fs^2, in good agreement with the theoretical expectation (1450 fs^2) calculated from a Sellmeier formula.

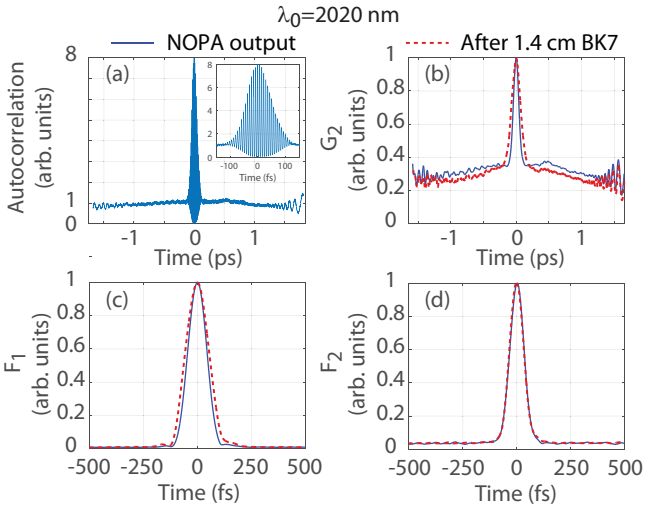

Figure 2. Autocorrelation obtained for a pulse at 2020 nm (a) and the associated oscillating function G_2 (b), F_1 (c), and F_2. The measurement of the pulse duration performed at the output of the NOPA is shown in blue while those done after propagation in a 1.4 cm BK7 plate is depicted in dashed red.

As discussed in the above section, F_2 can be used for estimating the laser spectrum. In order to confirm this, the spectrum retrieved with the autocorrelator has been compared with those actually measured with a commercial spectrometer (NIRQUEST from Ocean Optics) in the case of a laser pulse centered around λ_0=1820 nm. As shown in Fig.3, the spectrum estimated by the autocorrelator agrees well with the spectrum measured with the commercial spectrometer.

Usually, autocorrelators are sensitive to the input polarization. This is because almost autocorrelators are based on second-harmonic generation, which is a strongly polarization-dependent process. Accordingly, in such apparatus, the input pulse has to be linearly polarized in a particular direction. Since the presented autocorrelator is based on a different process (two-photon absorption), one can wonder which polarization has to be used during the measurement. The two-photon absorption process is *a priori* a polarization dependent process due to the tensor nature of the two-photon absorption cross-section.

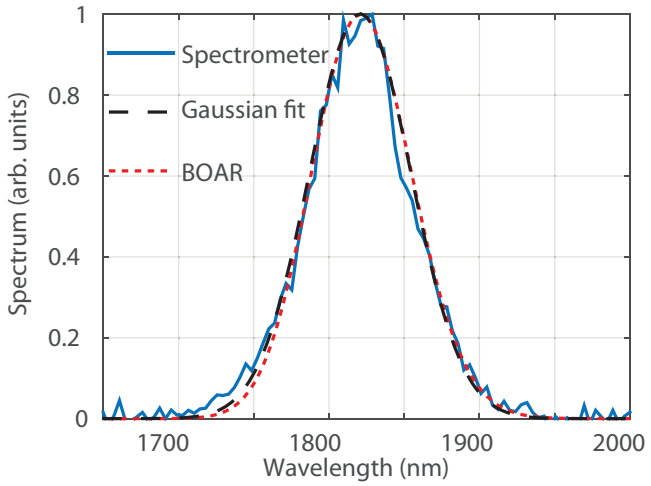

Figure 3. Laser spectrum measured with a commercial spectrometer (blue solid line) and evaluated with the BOAR (red dotted-dashed line). The black dashed line is a gaussian fit of the spectrum measured with the spectrometer. The central wavelength of the NOPA is set to 1820 nm.

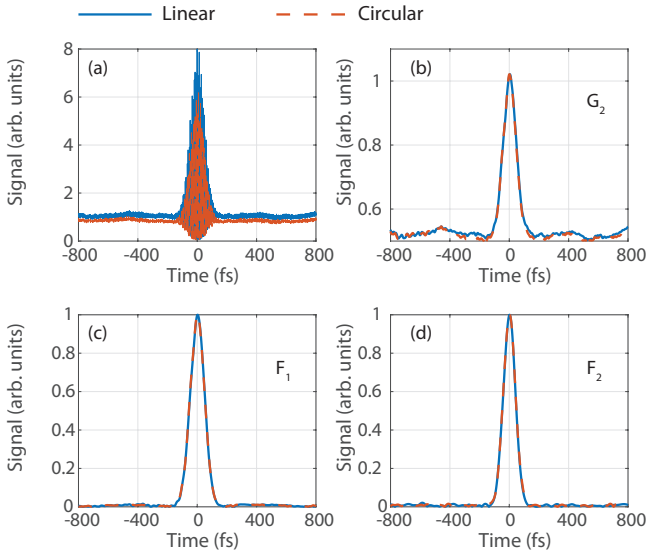

Figure 4. Comparison between experimental autocorrelations obtained for a linearly (dashed red) and circularly (solid blue) polarized pulse (a) and the associated oscillating functions G_2 (b), F_1 (c), and F_2 (d) in the case of a 1400 nm laser pulse.

In order to check the polarization dependence, a Berek compensator has been inserted before the autocorrelator. This compensator allows to impose any polarization to the pulse to be measured. The comparison between linear and circular polarizations is depicted in Fig. 4. Apart a slightly less intense signal obtained in the circular case, the two measured autocorrelations are almost identical and the fitting procedure gives the same results in both case. Note that the autocorrelator has been also tested in the cases of elliptical polarizations and gives the same result.

IV. FULL-SPATIO TEMPORAL DYNAMICS

Since the temporal characteristics of the pulse is transposed in the spatial domain, the spatial beam shape can affect the autocorrelation measurement. It is then of prime importance to characterize the spatio-temporal shape of the laser pulse in particular at the plane at which the camera is placed. To this end, full spatio-temporal propagation simulations have been performed so as, first, to validate the experimental protocol and, second, in order to quantify potential limitations of the autocorrelator. In order to mimic as close as possible the experimental configuration, a $H = 2\,\mathrm{cm}$ fused silica biprism with an 160° Apex angle has been considered. Accordingly, the expected delay range accessible with this biprism is about $\Delta\tau_{\max} = 5\,\mathrm{ps}$ and the optimal distance is $d_{\mathrm{opt}} \simeq 6.3\,\mathrm{cm}$. The central wavelength of the laser has been set to $\lambda_0 = 2\,\mu\mathrm{m}$. The spectrum $\widetilde{E}(x,\omega)$ of the electric field $E(x,t)$, chosen to be as close as possible to the experimental conditions presented here, reads in good approximation after the biprism:

$$\widetilde{E}(x,\omega,d=0) = E_0 \mathrm{e}^{-\frac{x^6}{\sigma_p^6}} \mathrm{e}^{-\frac{x^2}{\sigma_x^2}} \mathrm{e}^{-\frac{\sigma_t^2\omega^2}{4}} \mathrm{e}^{iK\omega^2} \mathrm{e}^{i\Phi(x,\omega)} \cos(\omega_0 t)\,. \tag{8}$$

The super-gaussian function (σ_p=0.98 cm) additionally superimposed to the spatial profile mimics the geometrical truncation induced by the biprism, the latter being smaller than the beam size (σ_x=3.4 cm) after its magnification by the cylindrical telescope. Finally, $\Phi(x,\omega)$ is the frequency-dependent phase introduced by propagation through the biprism. The latter reads:

$$\Phi(x,\omega) = n(\omega)\omega e(x)/c + \omega l(x)/c, \tag{9}$$

where $e(x)$ [resp. $l(x)$] is the thickness of the fused silica (resp. air) crossed by the ray arriving at a given height x at the output of the biprism:

$$\begin{aligned} e(x) &= \left(\frac{H}{2} - \frac{|x|}{1-\tan[\alpha(\omega)]\tan\beta}\right)\tan\beta, \\ l(x) &= |x|\frac{\sin\beta}{\cos[\alpha(\omega)+\beta]}. \end{aligned} \tag{10}$$

The introduced phase then takes into account the fact that the central part of the laser pulse experiences a stronger dispersion than the outer region because of a longer propagation path through the biprism. It also takes into account, through the frequency dependence of α, that the frequencies within the pulse spectrum are not deviated exactly with the same angle because of the refractive index dispersion. These two parameters are those limiting the measurement of very short laser pulses as it will be described below. In the case of small angle, after a propagation distance d in the air, the electric field becomes in the Fourier space:

$$\widetilde{E}(k_x,\omega,d) = \widetilde{E}(k_x,\omega,0)\mathrm{e}^{i\left[k_{\mathrm{air}}(\omega) - k_x^2/(2k_{\mathrm{air}}(\omega))\right]d}, \tag{11}$$

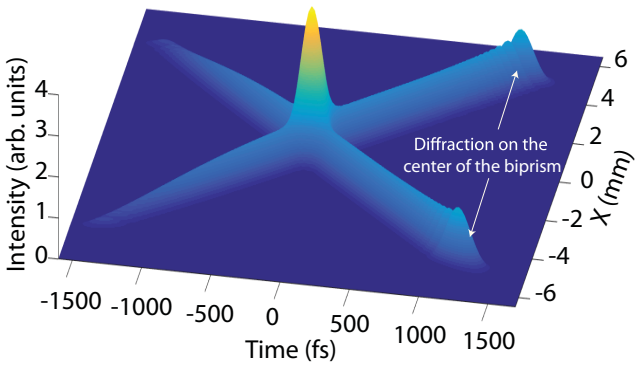

Figure 5. Spatio-temporal distribution of the pulse intensity at $d = d_{\rm opt}$.

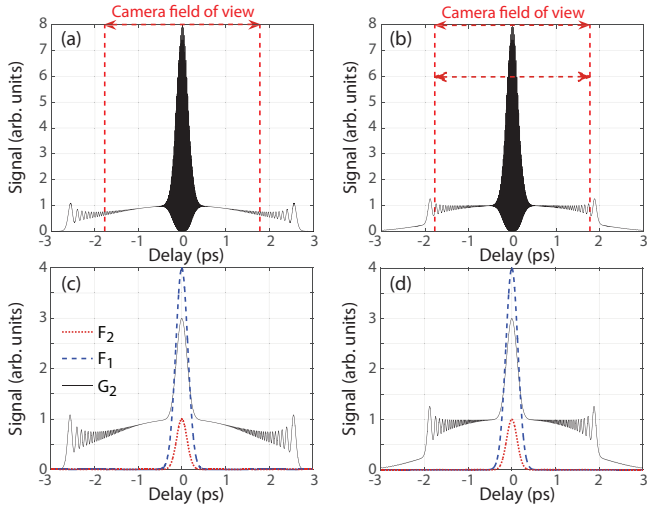

Figure 6. Typical theorical autocorrelation signal obtained by two-photon absorption with a 160° fused silica biprism (a) placed at the optimal distance ($d_{\rm opt}$ = 6.3 cm) and (b) where the biprism is placed experimentally (d = 4.7 cm) for a $\lambda = 2\mu$m, 100 fs pulse. The associated oscillating functions obtained after a spectral filtering are shown in (c) and (d) respectively.

where $k_{\rm air}(\omega) = n_{\rm air}(\omega)\omega/c$, k_x is the conjugate variable of x in the reciprocal space and $n_{\rm air}$ is the frequency-dependent refractive index of the air. The spatio-temporal distribution of the electric field $E(x, t, d)$ is then easily retrieved by an inverse Fourier-Transform in both space and time. Figure 5 shows the spatio-temporal distribution of the pulse intensity at $d = d_{\rm opt}$. The two parts of the beam coming from the two faces of the biprism intersect and interfere at the center because they temporally overlap. Note that the part of the energy located at positive times comes from the central edge of the biprism. Because of the discontinuity, it experiences diffraction so that oscillations can be noticed in the spatial profile. The photocurrent induced by two-photon absorption is then calculated by using Eq. 1 as exemplified in Fig. 6(a) for $d = d_{\rm opt}$ = 6.3 cm in the case of a $\lambda_0 = 2\,\mu$m 100 fs Fourier transform limited laser pulse. Then, the three oscillating functions F_2, F_1, and G_2 are isolated by a spectral filtering [Fig. 6(c)] and fitted using Eqs. 6. As explained earlier, working at $d = d_{\rm opt}$ provides the largest temporal window. However, because of the gaussian spatial profile, the offset is not uniform at this distance, which can be detrimental to correctly fit G_2 using Eq. 6. For solving this issue and since the camera size actually limits the duration range that can be measured, a slightly shorter distance (d = 4.7 cm) was chosen experimentally so as to obtained a flat offset over the full temporal window. The numerical two-photon absorption signal obtained in this case and the associated oscillating functions are shown in Figs. 6(b) and (d), respectively. Finally, the output of the propagation code has been compared to the experiments (see Fig. 7). The pulse parameter chosen in the simulation are those retrieved by the fit procedure during the experiment ($\Delta t_{\rm FTL}$ =57 fs and Δt=77 fs). As shown, the simulation is in excellent agreement with the experiment, which then validates the propagation code.

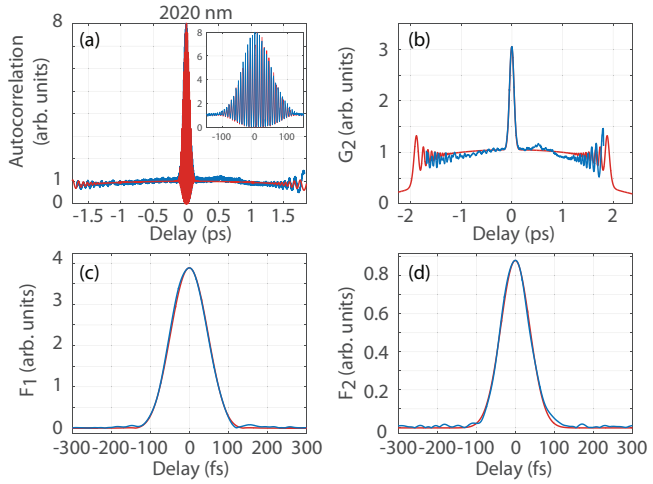

Figure 7. Comparison between the propagation code (red) and the experiment (blue). The Fourier-Transform limited (resp. chirped) pulse duration of the pulse is 57 (resp. 77) fs. The central wavelength is 2020 nm.

A. Limitations of the autocorrelator

1. Pulse durations working range

Two distinct factors limit the pulse duration range that can be measured by means of the presented autocorrelator. The minimal FTL pulse duration that can be measured is limited by the group velocity dispersion occurring during the propagation through the biprism. In the case of a Fourier transform limited pulse, the propaga-

tion within the biprism will make the pulse longer. More particularly, it can be shown that the quadratic phase introduced by the biprism Φ_p is in good approximation

$$\Phi_p = \frac{k^{(2)}(\omega_0)}{2}\omega^2 e_{\text{eff}}, \tag{12}$$

where $k^{(2)}(\omega_0) = \partial^2 k/\partial\omega^2(\omega_0)$ is the group velocity dispersion of the biprism material, $e_{\text{eff}} = e_0\left(1 - \frac{d}{2d_{\text{opt}}}\right)$ is the effective thickness of the biprism and $e_0 = \frac{H}{2}\tan\beta$ is the thickness of the biprism at the center. The propagation code described above was used to quantify the minimal and maximal pulse durations that can be measured with our autocorrelator. For a given and known initial set of parameters (FTL pulse duration and frequency chirp), the autocorrelation signal was numerically evaluated, giving in turn the three contributions G_2, F_1 and F_2 after an appropriate spectral filtering. Then, these extracted contributions were fitted as it is done in experiments. The resulting fits then give access to the *evaluated* FTL pulse duration and frequency chirp, which can be compared to the initial set of parameters. The difference between the initial conditions and the fit of the parameters then gives the error introduced by the measurement apparatus itself. Figure 9(a) shows the relative error made by the pulse duration measurement as a function of the input pulse duration (full width at half maximum) in the conditions used during our experiment. The measurement of F_2 (FTL pulse duration) is almost not affected by the propagation through the biprism. This is because F_2 is insensitive to the chirp, and consequently, to the group velocity dispersion induced in the biprism. In fact, the only thing that introduces an error is the frequency-dependence of the refraction angle at the biprism output leading to an angular chirp. However, this effect remains marginal for pulses longer than 15 fs if a fused silica biprism is used. On the contrary, the retrieved chirped pulse duration (using either G_2 or F_1) is longer than expected, in particular, for very short pulses and well fits the duration expected if one considers the dispersion induced by the propagation within the biprism. This means that the main effect introducing an error in the pulse measurement comes from the dispersion introduced by the propagation within the biprism and can be easily compensated during the fit algorithm. If the tolerance is set to 10 %, the minimal pulse duration that can be measured in this condition (i.e., with a fused silica biprism) is about 25 fs. More particularly, setting a 10 % tolerance in the pulse duration measurement and considering the biprism-induced groupe velocity dispersion only, one can show that the minimal pulse duration (FWHM) measurable with the present setup is given by:

$$\Delta_{t_{min}}(\omega_0) = 2\sqrt{\log(2)k^{(2)}(\omega_0)e_{\text{eff}}}\left(1.1^2 - 1\right)^{1/4}. \tag{13}$$

Since the group-velocity dispersion of the biprism is not constant over the full spectral window, the minimal pulse duration depends on the pulse central wavelength to be measured (Fig. 8). Note that, this limit can be pushed below by the use of a NaCl biprism instead of a fused silica biprism because the former has a smaller group velocity dispersion beyond 1.6 μm. Note also that these calculations do not take into account the finite spectral extension of the two-photon absorption band. In particular, close to the upper and lower limit of the band, the minimal pulse duration measurable with our autocorrelator will be limited by the fact that a part of the pulse spectrum goes beyond the spectral region of two-photon absorption. Figure 9(b) shows the error made when such a biprism is used (the apex angle of the latter has been chosen so as to keep the same deviation angle). In this case, the minimal pulse duration measurable is about 11 fs. As far as the maximal measurable FTL pulse duration is concerned, it is limited by the finite spatial expansion of the laser beam and does not depend on the biprism material as it can be noticed by comparing Fig. 9(a) and Fig. 9(b) in the long pulse region. In the chosen configuration, the maximal pulse duration that can be measured is about 1 ps (FWHM) when using G_2 and slightly more ($\simeq 1.5$ ps) when using the combination of F_1 and F_2. This difference is due to the fact that the quality of the fit of G_2 does depend on the offset flatness while these of F_1 and F_2 do not. In the case of a chirped laser pulse to be measured, the group delay dispersion induced by the propagation through the biprism impacts the retrieval of the real pulse duration while the FTL pulse duration retrieval by means of F_2 remains accurate. Indeed, the quadratic phase after propagation within the biprism Φ_p is:

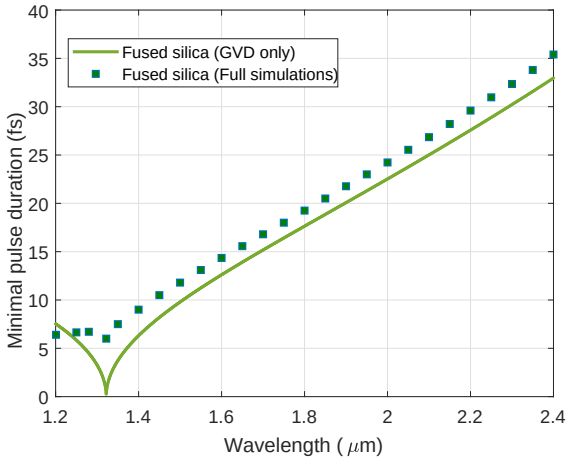

Figure 8. Theoretical minimal pulse duration measurable with the present autocorrelator as a function of the pulse central wavelength if one only considers the group velocity dispersion of the biprism (solid green line) and according to the full simulations (green squares).

$$\Phi_p = \left(K + \frac{k^{(2)}(\omega_0)}{2}e_{\text{eff}}\right)\omega^2, \tag{14}$$

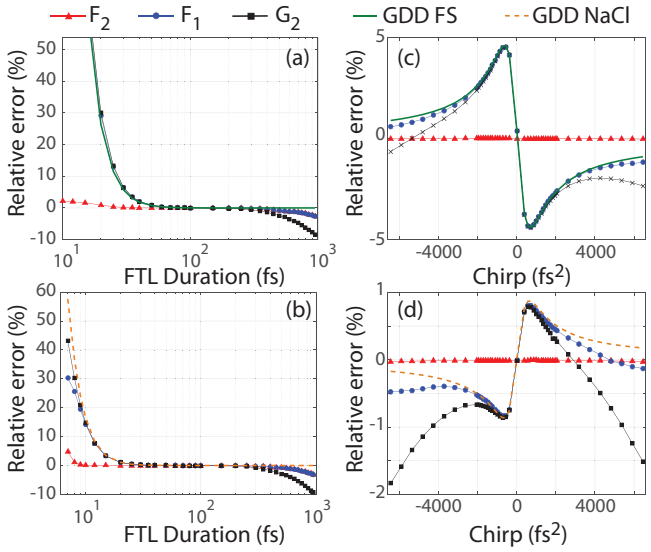

Figure 9. Relative error made by the fit as a function of the FTL pulse duration in the case of a fused silica (a) and NaCl (b) prism. Relative error made by the fit as a function of the initial chirp in the case of a fused silica (c) and NaCl (d) prism for a 60 fs laser pulse. The central wavelength of the pulse is 2 μm.

where K is the quadratic phase parameter of the pulse to be measured. Depending on the relative sign of K and the group delay dispersion introduced by the biprism, the chirped pulse duration effectively measured by the autocorrelator will be either longer or shorter than the pulse duration of the input pulse. Figures 9(c,d) show the relative error of the estimation as a function of K for a 60 fs (FWHM) 2μm laser pulse when using a fused silica or a NaCl biprism. For small K, the error is well fitted by the error introduced by the biprism dispersion. In the highly chirped case, however, the limiting factor is not the group velocity dispersion of the biprism but the finite spatial extension of the laser beam. As it is the case for FTL laser pulse, the use of G_2 for estimating the laser pulse duration leads to underestimate the pulse duration in this case. Note also that the use of a NaCl biprism leads to a smaller error on the pulse estimation also in this case. It then seems that NaCl should be preferred for the design of the autocorrelator. However, apart from the case of very short pulses (<20 fs), fused silica biprism remains a good choice, in particular if one takes into account that the fact that NaCl biprisms are much more costly than silica one.

2. Impact of the spatial quality of the beam

Another experimental parameter affecting the accuracy of a single-shot autocorrelator is the spatial beam quality. Indeed, since the temporal information is transposed in the spatial domain, the presence of noise in the spatial domain in turn degrades the quality of the pulse duration retrieval. In order to estimate the error made when dealing with a noisy laser beam, simulations have been performed with spatial transverse profiles on which different noise amplitudes have been superimposed. The noise used in the simulation has not been chosen as a completely random function but behaves as $1/k_x$ (where k_x is the spatial frequency), i.e., a low frequency spatial noise. This choice reproduces somehow the behavior of the noise effectively affecting amplified laser pulses as it has also been verified with our own laser system. Figure 10 shows the relative error made by the fitting procedure for different noise amplitudes (keeping constant the noise spatial shape) as a function of the chirp amplitude for a 60 fs 2 μm laser pulse. The spatial profile of the electric field used in the three cases are depicted in the insets. As expected, the presence of noise is detrimental for the pulse duration retrieval. At low noise amplitude [Fig. 10(a)], the error remains limited by the dispersion and finite spatial extend of the laser pulse. This is not the case anymore for intermediate and strong noise amplitudes. It can be noticed that F_2 is almost unaffected by the presence of noise unlike F_1 and G_2. There are two different reasons explaining the different impact of the noise on the fit accuracy. First, one has to remember that G_2, F_1 and F_2 evolve around $\omega = 0$, $\omega = \omega_0$ and $\omega = 2\omega_0$, respectively. This difference on the temporal domain is transposed in the spatial domain by the use of the biprism. Since the noise mostly affects the low spatial frequency, it impacts more G_2 than F_1 and leaves F_2 almost unaffected. The second reason explaining why F_2 is far less impacted than the two other functions is that G_2 and F_1 extend on a longer transverse dimension as the chirp parameter increases. As a consequence, they are more sensitive to the low-frequency spatial noise. Finally, as discussed above, the fit accuracy of F_1 decreases for long chirped laser pulse because this function tends to a chirp unsensitive function as the chirp increases. This is particularly true in presence of noise on the spatial profile. Note, however, that the impact of the noise can be decreased experimentally by a binning of the pixels over the vertical dimension, which is not used for pulse duration retrieval. This averaging can be directly performed in the hardware of the camera and/or a software-performed averaging over the vertical dimension of the two-photon absorption signal. As shown in Figs. 10, the presence of noise in the spatial profile mostly impacts the accuracy of the fit of G_2, mainly because the fitting procedure of the latter is strongly dependent on the offset flatness.

V. EXTENSION OF THE PRINCIPLE AT LONGER WAVELENGTHS

As explained above, using a silicon camera allows to measure pulse durations for pulses located between 1200 nm and 2400 nm, which is the wavelength range of two-photons absorption of the silicon. Measuring pulse

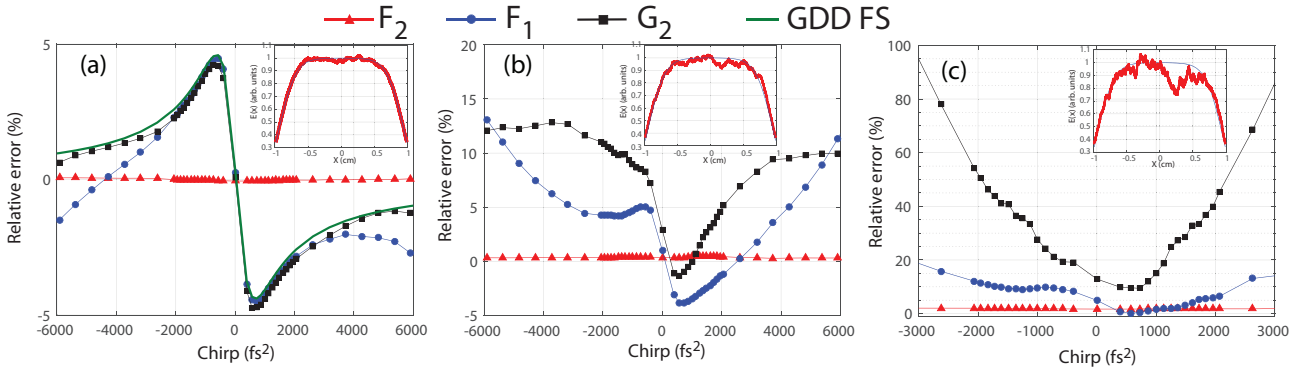

Figure 10. Relative error made by the fit as a function of the initial chirp in presence of a low (a), intermediate (b) and strong (c) noise in the spatial profile for a fused silica 160° biprism. The central wavelength of the pulse is 2 μm and the FTL pulse duration is 60 fs. The associated spatial electric field profile is shown in the subpanels.

duration of pulses located at higher wavelengths needs to adapt the materials composing the detector. A proof-of-principle experiment was performed by using a InGaAs camera (Goldeye G-033 from Allied Vision). The camera sensor is composed by 640x512 15 μm pixels. The NaCl Fresnel biprism used in this experiment has a 175° Apex angle. Figure 11(a) shows the two-photons absorption signal recorded by the camera in the case of a 3.1 μm femtosecond laser. As shown in Fig. 11(b) that displays the Fourier-Transform of the signal, the three contributions G_2, F_1, and F_2 clearly appears, which confirms the two-photons nature of the process. By fitting the oscillating functions F_1 and F_2 [see Fig. 11(c)], the pulse is found to be almost Fourier-Transform limited with a duration of approximatively 95 fs.

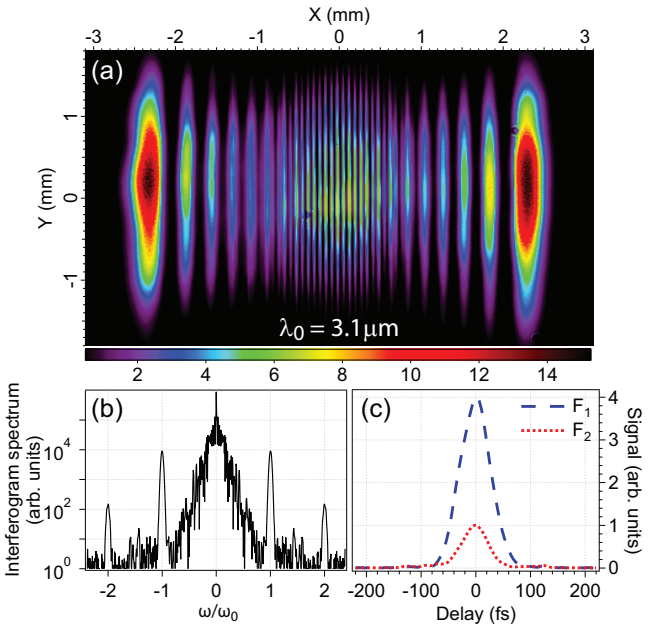

Figure 11. Pulse measurement performed at λ_0=3.1 μm with a InGaAs camera. (a) Two-photons absorption signal captured with the InGaAs camera. (b) Fourier-Transform of the two-photons signal showing the three different contributions oscillating at ω=0, ω_0, and $2\omega_0$, respectively. (c) Temporal distribution of F_1 and F_2. The retrieved pulse duration is about 95 fs.

VI. CONCLUSION

As a conclusion, a simple and compact single-shot autocorrelator based on two-photon absorption in a camera and working in the 1.2-2.4 μm spectral region has been presented and analyzed in details. The use of a Fresnel biprism for generating the two-replicas makes the autocorrelator extremely robust in alignment. Moreover, it has been shown that the autocorrelator is insensitive to the input pulse polarization contrary to almost all existing autocorrelators. The interferometric nature of the autocorrelator allows also to extract more information than a conventional intensimetric autocorrelator. In particular, it has been shown that the pulse spectrum, the frequency chirp and the pulse duration can be retrieved if ones assumes a particular temporal shape. Using a propagation code, the limitations of the autocorrelator have been analyzed. In particular, using a fused silica biprism, it has been shown that the pulse duration range accessible with the presented configuration extends from 25 fs to about 1 ps. Note that the lower limit can even be lowered by using a NaCl biprism instead of a fused silica one or by using a bimirror instead of a Fresnel biprism (i.e., by using an all-reflective geometry). Finally, the extension to higher wavelengths (up to 3.4 μm) has been demonstrated by substituting the silicon camera by a InGaAs one.

ACKNOWLEDGMENTS

This work was supported by the Conseil Régional de Bourgogne (PARI program), the CNRS, the SATT Grand-Est, and Carnot-ARTS. We thank the CRM-ICB

(Brice Gourier, Julien Lopez and Jean-Marc Muller) for the mechanical realization of the autocorrelator and the CRI-CCUB for CPU loan on the multiprocessor server.

REFERENCES

[1]Canhota, M., Silva, F., Weigand, R. and Crespo, H. M. Inline self-diffraction dispersion-scan of over octave-spanning pulses in the single-cycle regime. Opt. Lett. **42**, 3048-3051 (2017).

[2]Pulse retrieval algorithm for interferometric frequency-resolved optical gating based on differential evolution: Review of Scientific Instruments: **88**, No 10. (2017). Available at: http://aip.scitation.org/doi/abs/10.1063/1.4991852. (Accessed: 2nd January 2018)

[3]Shen, X., Wang, P., Liu, J., Kobayashi, T. and Li, R. Self-Referenced Spectral Interferometry for Femtosecond Pulse Characterization. Appl. Sci. **7**, 407 (2017).

[4]Prade, B. S., Schins, J. M., Nibbering, E. T. J., Franco, M. A. and Mysyrowicz, A. A simple method for the determination of the intensity and phase of ultrashort optical pulses. Opt. Commun. **113**, 79-84 (1994).

[5]Prein, S., Diddams, S. and Diels, J.-C. Complete characterization of femtosecond pulses using an all-electronic detector. Opt. Commun. **123**, 567-573 (1996).

[6]Lai, M. and Diels, J.-C. Complete diagnostic of ultrashort pulses without nonlinear process. Opt. Commun. **88**, 319.325 (1992).

[7]Diels, J.-C. M., Fontaine, J. J., McMichael, I. C. and Simoni, F. Control and measurement of ultrashort pulse shapes (in amplitude and phase) with femtosecond accuracy. Appl. Opt. **24**, 1270-1282 (1985).

[8]Ripoche, J.-F. et al. Determination of the duration of UV femtosecond pulses. Opt. Commun. **134**, 165-170 (1997).

[9]Chilla, J. L. A. and Martinez, O. E. Frequency domain phase measurement of ultrashort light pulses. Effect of noise. Opt. Commun. **89**, 434-440 (1992).

[10]Coello, Y. et al. Interference without an interferometer: a different approach to measuring, compressing, and shaping ultrashort laser pulses. JOSA B **25**, A140-A150 (2008).

[11]Zeylikovich, I. et al. Interferometric 2D imaging amplitude correlator for ultrashort pulses. Opt. Commun. **115**, 485-490 (1995).

[12]Stibenz, G. and Steinmeyer, G. Interferometric frequency-resolved optical gating. Opt. Express **13**, 2617-2626 (2005).

[13]Langlois, P. and Ippen, E. P. Measurement of pulse asymmetry by three-photon-absorption autocorrelation in a GaAsP photodiode. Opt. Lett. **24**, 1868-1870 (1999).

[14]Bender, D. A. and Sheik-Bahae, M. Modified spectrum autointerferometric correlation (MOSAIC) for single-shot pulse characterization. Opt. Lett. **32**, 2822.2824 (2007).

[15]Nicholson, J. W. and Rudolph, W. Noise sensitivity and accuracy of femtosecond pulse retrieval by phase and intensity from correlation and spectrum only (PICASO). JOSA B **19**, 330-339 (2002).

[16]Rhee, J.-K., Sosnowski, T. S., Tien, A.-C. and Norris, T. B. Real-time dispersion analyzer of femtosecond laser pulses with use of a spectrally and temporally resolved upconversion technique. JOSA B **13**, 1780-1785 (1996).

[17]Nibbering, E. T. J. et al. Spectral determination of the amplitude and the phase of intense ultrashort optical pulses. JOSA B **13**, 317-329 (1996).

[18]Sharma, A. K., Naik, P. A. and Gupta, P. D. The effect of errors and detector noise on sensitive detection of chirp and pulse asymmetry of ultrashort laser pulses from interferometric autocorrelation signals. Opt. Commun. **259**, 350-359 (2006).

[19]Bender, D. A., Nicholson, J. W. and Sheik-Bahae, M. Ultrashort laser pulse characterization using modified spectrum autointerferometric correlation (MOSAIC). Opt. Express **16**, 11782-11794 (2008).

[20]Yellampalle, B., Averitt, R. D. and Taylor, A. J. Unambiguous chirp characterization using modified-spectrum autointerferometric correlation and pulse spectrum. Opt. Express **14**, 8890-8899 (2006).

[21]Nicholson, J. W., Mero, M., Jasapara, J. and Rudolph, W. Unbalanced third-order correlations for full characterization of femtosecond pulses. Opt. Lett. **25**, 1801-1803 (2000).

[22]Karkhanehchi, M. M., Hamilton, C. J. and Marsh, J. H. Autocorrelation measurements of modelocked Nd:YLF laser pulses using two-photon absorption waveguide autocorrelator. IEEE Photonics Technol. Lett. **9**, 645.647 (1997).

[23]Spielmann, C., Xu, L. and Krausz, F. Measurement of interferometric autocorrelations: comment. Appl. Opt. **36**, 2523-2525 (1997).

[24]Choi, K. N. and Taylor, H. F. Novel crosscorrelation technique for characterization of subpicosecond pulses from modelocked semiconductor lasers. Appl. Phys. Lett. **62**, 1875-1877 (1993).

[25]Kane, D. J. and Trebino, R. Characterization of arbitrary femtosecond pulses using frequencyresolved optical gating. IEEE J. Quantum Electron. **29**, 571-579 (1993).

[26]DeLong, K. W., Trebino, R., Hunter, J. and White, W. E. Frequency-resolved optical gating with the use of second-harmonic generation. JOSA B **11**, 2206-2215 (1994).

[27]DeLong, K. W. and Trebino, R. Improved ultrashort pulse-retrieval algorithm for frequencyresolved optical gating. JOSA A **11**, 2429-2437 (1994).

[28]Paye, J., Ramaswamy, M., Fujimoto, J. G. and Ippen, E. P. Measurement of the amplitude and phase of ultrashort light pulses from spectrally resolved autocorrelation. Opt. Lett. **18**, 1946-1948 (1993).

[29]Kane, D. J., Taylor, A. J., Trebino, R. and DeLong, K. W. Single-shot measurement of the intensity and phase of a femtosecond UV laser pulse with frequency-resolved optical gating. Opt. Lett. **19**, 1061-1063 (1994).

[30]Kane, D. J. and Trebino, R. Single-shot measurement of the intensity and phase of an arbitrary ultrashort pulse by using frequency-resolved optical gating. Opt. Lett. **18**, 823-825 (1993).

[31]Peatross, J. and Rundquist, A. Temporal decorrelation of short laser pulses. JOSA B **15**, 216-222 (1998).

[32]Amat-Roldan, I., Cormack, I. G., Loza-Alvarez, P., Gualda, E. J. and Artigas, D. Ultrashort pulse characterisation with SHG collinear-FROG. Opt. Express **12**, 1169-1178 (2004).

[33]Bates, P. K., Chalus, O. and Biegert, J. Ultrashort pulse characterization in the mid-infrared. Opt. Lett. **35**, 1377-1379 (2010).

[34]Trebino, R. and Kane, D. J. Using phase retrieval to measure the intensity and phase of ultrashort pulses: frequency-resolved optical gating. JOSA A **10**, 1101-1111 (1993).

[35]Iaconis, C. and Walmsley, I. A. Spectral phase interferometry for direct electric-field reconstruction of ultrashort optical pulses. Opt. Lett. **23**, 792-794 (1998).

[36]Wong, V. and Walmsley, I. A. Analysis of ultrashort pulse-shape measurement using linear interferometers. Opt. Lett. **19**, 287-289 (1994).

[37]Wong, V. and Walmsley, I. A. Linear filter analysis of methods for ultrashort-pulse-shape measurements. JOSA B **12**, 1491-1499 (1995).

[38]Lepetit, L., Cheriaux, G. and Joffre, M. Linear techniques of phase measurement by femtosecond spectral interferometry for applications in spectroscopy. JOSA B **12**, 2467-2474 (1995).

[39]Ventalon, C., Fraser, J. M. and Joffre, M. Time-domain interferometry for direct electric field reconstruction of mid-infrared femtosecond pulses. Opt. Lett. **28**, 1826-1828 (2003).

[40]Fan, G. et al. X-SEA-F-SPIDER characterization of over octave spanning pulses in the infrared range. Opt. Express **24**, 12713-12729 (2016).

[41]Tokunaga, E., Terasaki, A. and Kobayashi, T. Induced phase modulation of chirped continuum pulses studied with a femtosecond frequency-domain interferometer. Opt. Lett. **18**, 370-372 (1993).

[42]Geindre, J. P. et al. Frequency-domain interferometer for measuring the phase and amplitude of a femtosecond pulse probing a laser-produced plasma. Opt. Lett. **19**, 1997-1999 (1994).
[43]Kovacs, A. P., Osvay, K., Bor, Z. and Szipocs, R. Group-delay measurement on laser mirrors by spectrally resolved white-light interferometry. Opt. Lett. **20**, 788-790 (1995).
[44]Reynaud, F., Salin, F. and Barthelemy, A. Measurement of phase shifts introduced by nonlinear optical phenomena on subpicosecond pulses. Opt. Lett. **14**, 275-277 (1989).
[45]Kleimeier, N. F. et al. Autocorrelation and phase retrieval in the UV using two-photon absorption in diamond pin photodiodes. Opt. Express **18**, 6945-6956 (2010).
[46]Danielius, R., Stabinis, A., Valiulis, G. and Varanavi.ius, A. Characterization of phase modulated ultrashort pulses using single-shot autocorrelator. Opt. Commun. **105**, 67-72 (1994).
[47]Goodberlet, J. and Hagelstein, P. L. Chirp-compensated autocorrelation of optical pulses. Opt. Lett. **18**, 1648-1650 (1993).
[48]DeLong, K. W. and Yumoto, J. Chirped light and its characterization using the cross-correlation technique. JOSA B **9**, 1593-1607 (1992).
[49]Nicholson, J. W., Jasapara, J., Rudolph, W., Omenetto, F. G. and Taylor, A. J. Full-field characterization of femtosecond pulses by spectrum and cross-correlation measurements. Opt. Lett. **24**, 1774-1776 (1999).
[50]Gebert, T. et al. Michelson-type all-reflective interferometric autocorrelation in the VUV regime. New J. Phys. **16**, 073047 (2014).
[51]Chen, C.-W., Huang, J. Y. and Pan, C.-L. Pulse retrieval from interferometric autocorrelation measurement by use of the population-split genetic algorithm. Opt. Express **14**, 10930-10938 (2006).
[52]Yang, W. et al. Spectral phase retrieval from interferometric autocorrelation by a combination of graduated optimization and genetic algorithms. Opt. Express **18**, 15028-15038 (2010).
[53]Kane, D. J. Real-time measurement of ultrashort laser pulses using principal component generalized projections. IEEE J. Sel. Top. Quantum Electron. **4**, 278-284 (1998).
[54]Sidorenko, P., Lahav, O., Avnat, Z. and Cohen, O. Ptychographic reconstruction algorithm for frequency-resolved optical gating: super-resolution and supreme robustness. Optica **3**, 1320. 1330 (2016).
[55]On the Uniqueness of FROG Methods - IEEE Journals & Magazine. Available at: http://ieeexplore.ieee.org/abstract/document/7891012/. (Accessed: 2nd January 2018)
[56]Oksenhendler, T. et al. Self-referenced spectral interferometry. in 2009 Conference on Lasers and Electro-Optics and 2009 Conference on Quantum electronics and Laser Science Conference 1.2 (2009). doi:10.1364/CLEO.2009.CThW4
[57]Yasa, Z. A. and Amer, N. M. A rapid-scanning autocorrelation scheme for continuous monitoring of picosecond laser pulses. Opt. Commun. **36**, 406-408 (1981).
[58]Chuzavkov, Y. L. et al. Single-shot autocorrelator. in 3516, 743-746 (International Society for Optics and Photonics, 1999).
[59]Brun, A., Georges, P., Saux, G. L. and Salin, F. Single-shot characterization of ultrashort light pulses. J. Phys. Appl. Phys. **24**, 1225 (1991).
[60]Liesfeld, B., Bernhardt, J., Amthor, K.-U., Schwoerer, H. and Sauerbrey, R. Single-shot autocorrelation at relativistic intensity. Appl. Phys. Lett. **86**, 161107 (2005).
[61]Zhang, Y. et al. Single-shot, real-time carrier-envelope phase measurement and tagging based on stereographic above-threshold ionization at short-wave infrared wavelengths. Opt. Lett. **42**, 5150-5153 (2017).
[62]Manzoni, C., Forst, M., Ehrke, H. and Cavalleri, A. Single-shot detection and direct control of carrier phase drift of midinfrared pulses. Opt. Lett. **35**, 757-759 (2010).
[63]Dubrouil, A. et al. Spatio.spectral structures in high-order harmonic beams generated with Terawatt 10-fs pulses. Nat. Commun. **5**, 4637 (2014).
[64]Feng, C. et al. Complete analog control of the carrier-envelope-phase of a high-power laser amplifier. Opt. Express **21**, 25248-25256 (2013).